GLOBAL GEOMETRIC PROPERTIES OF MARTIAN IMPACT CRATERS: A PRELIMINARY ASSESSMENT USING MARS ORBITER LASER ALTIMETER (MOLA). J. B. Garvin[1], S. E. H. Sakimoto[2], C. Schnetzler[3], and J. J. Frawley[4], [1](NASA's GSFC, Code 921, Greenbelt, MD 20771 USA; garvin@denali.gsfc.nasa.gov), [2](USRA at NASA's GSFC, Code 921, Greenbelt, MD 20771), [3](SSAI at NASA's GSFC) [4](H-STX and Herring Bay Geophysics at NASA's GSFC).

Introduction: Impact craters on Mars have been used to provide fundamental insights into the properties of the martian crust, the role of volatiles, the relative age of the surface, and on the physics of impact cratering in the Solar System [1,2,6]. Before the three-dimensional information provided by the Mars Orbiter Laser Altimeter (MOLA) instrument which is currently operating in Mars orbit aboard the Mars Global Surveyor (MGS), impact features were characterized morphologically using orbital images from Mariner 9 and Viking. Fresh-appearing craters were identified and measurements of their geometric properties were derived from various image-based methods [3,6]. MOLA measurements can now provide a global sample of topographic cross-sections of martian impact features as small as ~ 2 km in diameter, to basin-scale features. We have previously examined MOLA cross-sections of Northern Hemisphere [4] and North Polar Region impact features [5], but were unable to consider the global characteristics of these ubiquitous landforms. Here we present our preliminary assessment of the geometric properties of a globally-distributed sample of martian impact craters, most of which were sampled during the initial stages of the MGS mapping mission (i.e., the first 600 orbits). Our aim is to develop a framework for reconsidering theories concerning impact cratering in the martian environment. This first global analysis is focused upon topographically-fresh impact craters, defined here on the basis of MOLA topographic profiles that cross the central cavities of craters that can be observed in Viking-based MDIM global image mosaics. We have considered crater depths, rim heights, ejecta topologies, cross-sectional "shapes", and simple physical models for ejecta emplacement [4]. To date (May, 1999), we have measured the geometric properties of over 1300 impact craters in the 2 to 350 km diameter size interval. A large fraction of these measured craters were sampled with cavity-center cross-sections during the first two months of MGS mapping. Many of these craters are included in Nadine Barlow's Catalogue of Martian Impact Craters [2], although we have treated simple craters smaller than about 7 km in greater detail than all previous investigations.

MOLA Measurements: Using MOLA profile and gridded topographic data, we have measured a suite of more than 20 geometric properties for each topographically-fresh impact feature identified. Included in this array of derived properties are: depth d, rim height h, cavity volume V, ejecta volume V_e, ejecta flank slope, ejecta thickness function (ETF) exponent (b) and coefficient (a), inner cavity wall slope, cavity cross-sectional "shape" (n), central peak height, diameter D, volume, shape, and many others. In this report, we treat the crater depth versus diameter relationship, the crater rim height vs. diameter pattern, the statistics of ejecta thickness and its spatial distribution, and cavity geometric properties, including interior deposit geometry.

Crater depth vs. Diameter: Using MOLA topographic profile data, we have computed the total depth (from rim crest to lowest point on crater cavity floor) and true depth (i.e., from pre-impact surface to mean crater floor level) for over 1300 craters. When we examine the correlation of depth d against diameter D, a pattern emerges, as was first recognized by Pike and others for the Moon, Mars, and Mercury [6]. Crater depth decreases in somewhat discrete steps as a function of diameter and hence kinetic energy. This pattern is evident in MOLA-based data. When we employ non-linear least-squares regression methods to fit the d vs. D data to an equation of the form : $d = k D^z$, where k and z are fit constants, we can solve for the optimal k and z (i.e. those values with the highest correlation coefficient). We have used this approach to analyze the depth versus diameter distribution as a function of location on Mars globally, as well as on a regional basis (polar vs. non-polar). Natural break-points in the distribution are observed near 7 km (the so-called simple-to-complex transition) and again at ~ 90 km (the complex-to-proto-basin transition). For all craters between 70N and 70S (non-polar) we have 961 measurements of the central portion of their cavities. Such mid-latitude craters display depth-diameter behavior as follows:

$$d = 0.12D^{0.96} \quad \text{(simple: D < 7 km)}$$

$$d = 0.20D^{0.53} \quad \text{(complex: 7 < D < 90 km)}$$

$$d = 0.98D^{0.18} \quad \text{(proto-basins: D > 90 km),}$$

where the exponent (z) in each case has a standard error of ~0.04 and where d, D are measured in km. These non-polar latitude values are similar to those of Pike and Davis [3], who found $z = 0.504$ for complex craters larger than 6 km. The development of a depth versus diameter model for simple craters smaller than ~ 7 km is new, and suggests that local target effects may exert some influence on final crater depths at these kinetic energy levels. The "discovery" of a proto-basin transition near ~ 90 km for Mars has important implications. It suggests that large crater depth plateaus dramatically at diameters beyond 90 km. This may be caused by enhanced impact melt accumulation and fall-back or

cavity-wall slumping effects. Well-known large impact craters in the Northern hemisphere, including *Mie*, *Lomonosov*, *Kunowsky*, *Korolev*, and *Milankovic* are all in this "proto-basin" class. MOLA topographic cross-sections of these craters indicate substantial cavity infill, in some cases moderating their cavity floor topography and lessening the apparent depth. For example, 80-100 km diameter fresh-appearing craters in the polar regions such as Korolev and South display typical cavity interior deposits (Figure 1). In each of these cases, the infilling deposits constitute > 50% of the apparent crater cavity volume. This argues for a post-impact sedimentation event or events. The polar crater infilling deposits are commonly at a similar topographic level as the surrounding pre-impact surface.

Rim height (h), in correlation with crater diameter, follows a similar trend, in which $h \sim 0.03\ D^{0.96}$ for simple craters ($D < 7$ km), and $h \sim 0.06\ D^{0.51}$ for complex craters larger than 7 km. These relationships can also be used to assess regional flooding levels, following the approach pioneered by DeHon and others.

Cavity cross-section (n), here defined as the power in the exponential function that best describes the topographic cross-section of the crater cavity, is also correlated with diameter. For complex craters larger than about 7 km, $n \sim 1.63\ D^{0.11}$, while craters larger than about 75 km typically display n values that approach 3.0, because of cavity floor sedimentation. This suggests that the transition from complex to proto-basins on Mars is distinctive and occurs at diameters in excess of 75 km.

CONCLUSIONS: We have measured more than 1300 martian crater cavities and their associated ejecta blankets with MOLA topographic cross-sections and grids. This population of topographically "fresh" craters is globally representative and indicates that the North Polar region is **distinctive** as a target type in comparison with the rest of Mars. This work is in progress and development of geological unit based correlations is proceeding.

ACKNOWLEDGEMENTS: We are grateful for the strong support of the MGS project, of the MOLA PI's (D. Smith and M. Zuber), and for the efforts of Greg Neumann. The MOLA Engineering team facilitated measurement of impact craters on Mars since the instrument was designed in 1988 – we thank James Abshire, Jack Bufton, J. Bryan Blair, Ron Follas, Jay Smith, and Bert Johnson for their essential efforts.

References: [1] Carr M. H. (1977) JGR 82, 4055-4065. [2] Barlow N. and T. Bradley (1990) Icarus 87, 156-179. [3] Pike R. J. and P. Davis (1984) LPSC XVIII, [4] Garvin J. and J. Frawley, GRL 25, 4405-4408. 645-646. [5] Garvin J. B. et al. (1999) submitted to Icarus, 57 pp. [6] Pike R. J. (1980) Proc. LPSC 11th, 2159-2189.

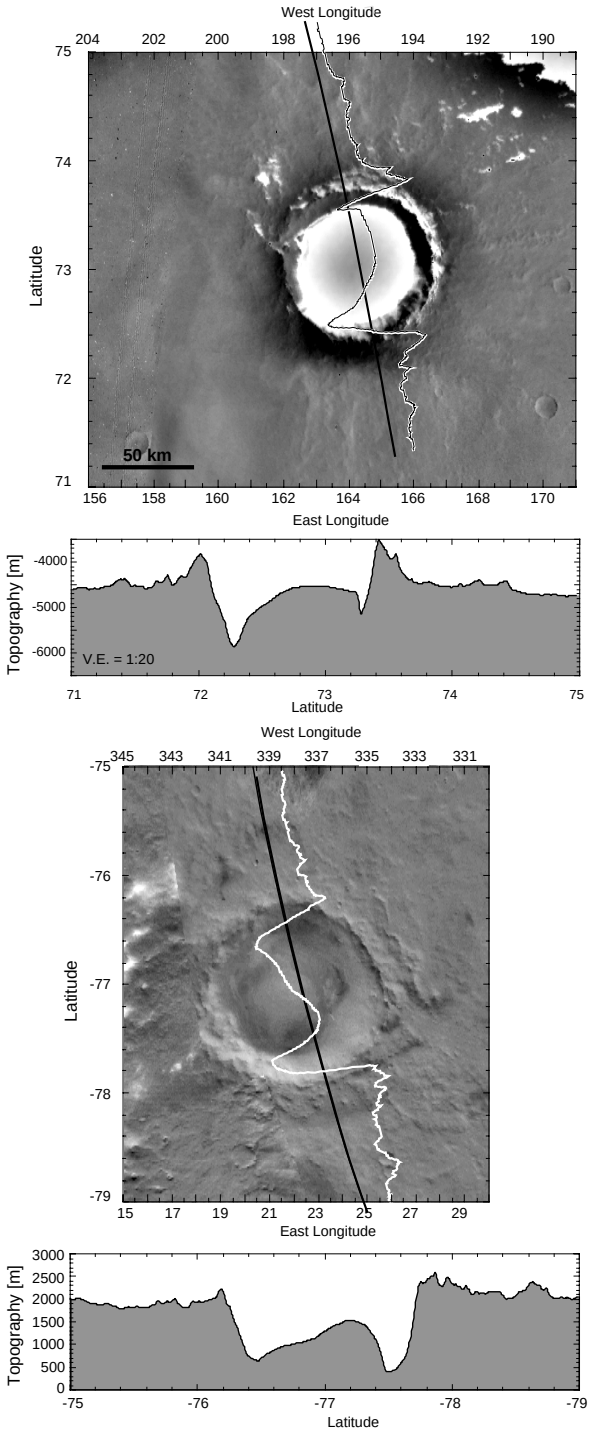

Figure 1. Viking MDIM Images and MOLA topography profiles of Korolev crater (top)and South crater (bottom). White traces on images are profiles with (black) track locations. Both craters have the unusually large cavity deposits typical of polar region craters in the MOLA topography.